immunity using a mouse model of septic peritonitis. It is striking that administration of diphenhydramine impaired morbidity in septic peritonitis, whereas desloratadine has no such effect. Notably, a lack of influence on the morbidity of peritonitis model using H1 receptor-null mice clearly indicated that diphenhydramine affected morbidity through some other pathway apart from H1 receptor-mediated signaling [78••]. Thus, although the detailed mechanism is unclear, older first-generation antihistamines potentially exacerbate skin allergies via increased risk of infection.

Conclusion

Antihistamines are well known therapeutic agents for improving the itch symptom or flare caused by the release of histamine from various types of cells, including mast cells and basophils. Actually, both older first-generation and more recent second-generation antihistamines reduce these symptoms successfully. However, the effects of these two types of antihistamine on daily living crucially differ from each other. From recent studies that evaluated patient QoL, we should focus on improving patients' activities involved in daily living, rather than merely decreasing symptoms of allergic diseases. From this perspective, second-generation antihistamines are recommended as a first-line treatment for skin allergies. In addition to H1 receptor antagonism, basic research on the function of second-generation antihistamines has revealed their unique properties, such as amelioration of ancillary symptoms found in skin allergies. Evaluation of reproducibility of such characteristics of these antihistamines in clinical practice should be performed in the future, and such information will contribute to improvements in both the status of antihistamines in the management of skin allergies and, most of all, patients' activity involved in daily living.

Acknowledgement

This work was supported by Health and Labour Sciences Research Grant of Japan.

Conflicts of interest

There are no conflicts of interest.

References and recommended reading

Papers of particular interest, published within the annual period of review, have been highlighted as:

- • of special interest
- •• of outstanding interest

Additional references related to this topic can also be found in the Current World Literature section in this issue (pp. 500–501).

1 Akdis CA, Simons FE. Histamine receptors are hot in immunopharmacology. Eur J Pharmacol 2006; 533:69–76.

2 Murota H, Katayama I. Emedastine difumarate: a review of its potential ameliorating effect for tissue remodeling in allergic diseases. Expert Opin Pharmacother 2009; 10:1859–1867.

3 Zuberbier T, Asero R, Bindslev-Jensen C, *et al.* EAACI/GA(2)LEN/EDF/WAO guideline: management of urticaria. Allergy 2009; 64:1427–1443.

4 Powell RJ, Du Toit GL, Siddique N, *et al.* BSACI guidelines for the management of chronic urticaria and angio-oedema. Clin Exp Allergy 2007; 37:631–650.

5 Tedeschi A, Girolomoni G, Asero R. AAITO Position paper. Chronic urticaria: diagnostic workup and treatment. Eur Ann Allergy Clin Immunol 2007; 39:225–231.

6 Joint Task Force on Practice Parameters. The diagnosis and management of urticaria: a practice parameter part I: acute urticaria/angioedema part II: chronic urticaria/angioedema. Joint Task Force on Practice Parameters. Ann Allergy Asthma Immunol 2000; 85:521–544.

7 Hide M, Furue M, Ikezawa Z, *et al.* Guidelines for the diagnosis and treatment of urticaria and angioedema [in Japanese]. Jpn J Dermatol 2005; 115:703–715.

8 Schulz S, Metz M, Siepmann D, *et al.* Antipruritic efficacy of a high-dosage antihistamine therapy: results of a retrospectively analysed case series. Hautarzt 2009; 60:564–568.

9 Williams HC. Clinical practice. Atopic dermatitis. N Engl J Med 2005; 352:2314–2324.

10 Klein PA, Clark RA. An evidence-based review of the efficacy of antihistamines in relieving pruritus in atopic dermatitis. Arch Dermatol 1999; 135:1522–1525.

11 Hanifin JM, Cooper KD, Ho VC, *et al.* Guidelines of care for atopic dermatitis, developed in accordance with the American Academy of Dermatology (AAD)/American Academy of Dermatology Association 'Administrative Regulations for Evidence-Based Clinical Practice Guidelines'. J Am Acad Dermatol 2004; 50:391–404.

12 Akdis CA, Akdis M, Bieber T, *et al.* Diagnosis and treatment of atopic dermatitis in children and adults: European Academy of Allergology and Clinical Immunology/American Academy of Allergy, Asthma and Immunology/PRACTALL Consensus Report. Allergy 2006; 61:969–987.

13 Lewis-Jones S, Mugglestone MA. Management of atopic eczema in children aged up to 12 years: summary of NICE guidance. BMJ 2007; 335:1263–1264.

14 Leung DY, Nicklas RA, Li JT, *et al.* Disease management of atopic dermatitis: an updated practice parameter. Joint Task Force on Practice Parameters. Ann Allergy Asthma Immunol 2004; 93:S1–S21.

15 Saeki H, Furue M, Furukawa F, *et al.* Guidelines for management of atopic dermatitis. J Dermatol 2009; 36:563–577.

16 Kawashima M, Tango T, Noguchi T, *et al.* Addition of fexofenadine to a topical corticosteroid reduces the pruritus associated with atopic dermatitis in a 1-week randomized, multicentre, double-blind, placebo-controlled, parallel-group study. Br J Dermatol 2003; 148:1212–1221.

17 Kawashima M, Harada S. Effect of standard medication on quality of life of patients with atopic dermatitis. J Dermatol 2007; 34:9–16.

18 Kawashima M, Harada S. A study of the effect on itch and quality of life of atopic dermatitis patients treated by standard therapy with antiallergic drug [in Japanese]. Jpn J Clin Dermatol 2006; 60:661–667.

19 Kobayashi M, Kabashima K, Nakamura M, *et al.* Downmodulatory effects of the antihistaminic drug bepotastine on cytokine/chemokine production and CD54 expression in human keratinocytes. Skin Pharmacol Physiol 2009; 22:45–48.

20 Xia Q, Yang S, Zhang SQ, *et al.* The effect of mizolastine on expression of vascular endothelial cell growth factor, tumour necrosis factor-alpha and keratinocyte-derived chemokine in murine mast cells, compared with dexamethasone and loratadine. Clin Exp Dermatol 2005; 30:165–170.

21 Giustizieri ML, Albanesi C, Fluhr J, *et al.* H1 histamine receptor mediates inflammatory responses in human keratinocytes. J Allergy Clin Immunol 2004; 114:1176–1182.

22 Kobayashi M, Kabashima K, Tokura Y. Inhibitory effects of epinastine on chemokine production and MHC class II/CD54 expression in keratinocytes. J Dermatol Sci 2007; 45:144–146.

23 Kobayashi M, Tokura Y. Preferential downmodulation of certain chemokines by fexofenadine in human keratinocytes. J Dermatol Sci 2005; 38:67–69.

24 Traidl-Hoffmann C, Munster I, Ring J, *et al.* Impact of desloratadine and loratadine on the crosstalk between human keratinocytes and leukocytes: implications for anti-inflammatory activity of antihistamines. Int Arch Allergy Immunol 2006; 140:315–320.

25 Shimizu T, Nishihira J, Watanabe H, *et al.* Cetirizine, an H1-receptor antagonist, suppresses the expression of macrophage migration inhibitory factor: its potential anti-inflammatory action. Clin Exp Allergy 2004; 34:103–109.

26 • Murota H, El-latif MA, Tamura T, *et al.* Olopatadine hydrochloride improves dermatitis score and inhibits scratch behavior in NC/Nga mice. Int Arch Allergy Immunol 2010; 153:121–132.

This literature is worth noting that an orally administered H1 receptor antagonist improved the diverse symptoms which are observed in atopic dermatitis model mice *in vivo*.

27 Sudofsky LR, Campi B, Trevisani M, *et al.* Transient receptor potential vanilloid-1-mediated calcium responses are inhibited by the alkylamine antihistamines dexbrompheniramine and chlorpheniramine. Exp Lung Res 2008; 34:681–693.

28 Massaad CA, Safieh-Garabedian B, Poole S, *et al.* Involvement of substance P, CGRP and histamine in the hyperalgesia and cytokine upregulation induced by intraplantar injection of capsaicin in rats. J Neuroimmunol 2004; 153:171–182.

29 Tamura T, Matsubara M, Amano T, *et al.* Olopatadine ameliorates rat experimental cutaneous inflammation by improving skin barrier function. Pharmacology 2008; 81:118–126.

30 Murota H, Bae S, Hamasaki Y, *et al.* Emedastine difumarate inhibits histamine-induced collagen synthesis in dermal fibroblasts. J Investig Allergol Clin Immunol 2008; 18:245–252.

31 Leonardi A, DeFranchis G, De Paoli M, *et al.* Histamine-induced cytokine production and ICAM-1 expression in human conjunctival fibroblasts. Curr Eye Res 2002; 25:189–196.

32 Asano K, Kanai K, Furuta A, *et al.* Suppressive activity of fexofenadine hydrochloride on nitric oxide production in vitro and in vivo. J Pharm Pharmacol 2007; 59:1389–1395.

33 De Luisi A, Mangialardi G, Ria R, *et al.* Antiangiogenic activity of carebastine: a plausible mechanism affecting airway remodelling. Eur Respir J 2009; 34:958–966.

34 Kitaba S, Murota H, Yahata Y, *et al.* Novel functional aspect of antihistamines: the impact of bepotastine besilate on substance p-induced events. J Allergy (Cairo) 2009; 2009:853687.

35 Vasiadi M, Kalogeromitros D, Kempuraj D, *et al.* Rupatadine inhibits proinflammatory mediator secretion from human mast cells triggered by different stimuli. Int Arch Allergy Immunol 2010; 151:38–45.

36 Matsubara M, Masaki S, Ohmori K, *et al.* Differential regulation of IL-4 expression and degranulation by antiallergic olopatadine in rat basophilic leukemia (RBL-2H3) cells. Biochem Pharmacol 2004; 67:1315–1326.

37 Asano K, Furuta A, Kanai K, *et al.* Inhibition of angiogenic factor production from murine mast cells by an antiallergic agent (epinastine hydrochloride) in vitro. Mediators Inflamm 2008; 2008:265095.

38 Wang YH, Tache Y, Harris AG, *et al.* Desloratadine prevents compound 48/80-induced mast cell degranulation: visualization using a vital fluorescent dye technique. Allergy 2005; 60:117–124.

39 Tokura Y, Kobayashi M, Ito T, *et al.* Antiallergic drug olopatadine suppresses murine contact hypersensitivity and downmodulates antigen-presenting ability of epidermal Langerhans cells. Cell Immunol 2003; 224:47–54.

40 Sugita K, Kabashima K, Tokura Y. Fexofenadine downmodulates antigen-presenting ability of murine epidermal Langerhans cells. J Dermatol Sci 2008; 49:88–91.

41 Sugita K, Kobayashi M, Mori T, *et al.* Antihistaminic drug olopatadine downmodulates CCL17/TARC production by keratinocytes and Langerhans cells. J Dermatol 2009; 36:654–657.

42 Wu P, Mitchell S, Walsh GM. A new antihistamine levocetirizine inhibits eosinophil adhesion to vascular cell adhesion molecule-1 under flow conditions. Clin Exp Allergy 2005; 35:1073–1079.

43 Mullol J, Roca-Ferrer J, Alobid I, *et al.* Effect of desloratadine on epithelial cell granulocyte-macrophage colony-stimulating factor secretion and eosinophil survival. Clin Exp Allergy 2006; 36:52–58.

44 Watase F, Watanabe S, Kanai K, *et al.* Modulation of eosinophil survival by epinastine hydrochloride, an H1 receptor antagonist, in vitro. In Vivo 2008; 22:687–691.

45 Hasala H, Moilanen E, Janka-Junttila M, *et al.* First-generation antihistamines diphenhydramine and chlorpheniramine reverse cytokine-afforded eosinophil survival by enhancing apoptosis. Allergy Asthma Proc 2007; 28:79–86.

46 Vancheri C, Mastruzzo C, Tomaselli V, *et al.* The effect of fexofenadine on expression of intercellular adhesion molecule 1 and induction of apoptosis on peripheral eosinophils. Allergy Asthma Proc 2005; 26:292–298.

47 Ikoma A, Steinhoff M, Stander S, *et al.* The neurobiology of itch. Nat Rev Neurosci 2006; 7:535–547.

48 Tominaga M, Tengara S, Kamo A, *et al.* Psoralen-ultraviolet A therapy alters epidermal Sema3A and NGF levels and modulates epidermal innervation in atopic dermatitis. J Dermatol Sci 2009; 55:40–46.

49 Heyer G, Hornstein OP, Handwerker HO. Skin reactions and itch sensation induced by epicutaneous histamine application in atopic dermatitis and controls. J Invest Dermatol 1989; 93:492–496.

50 Darsow U, Scharein E, Bromm B, *et al.* Skin testing of the pruritogenic activity of histamine and cytokines (interleukin-2 and tumour necrosis factor-alpha) at the dermal-epidermal junction. Br J Dermatol 1997; 137:415–417.

51 Davies MG, Greaves MW. Sensory responses of human skin to synthetic histamine analogues and histamine. Br J Clin Pharmacol 1980; 9:461–465.

52 Nishioka K, Katayama I, Doi T. Histamine release by scratching inflamed skin. J Dermatol 1987; 14:284–285.

53 Wahlgren CF. Itch and atopic dermatitis: an overview. J Dermatol 1999; 26:770–779.

54 Matsubara M, Tamura T, Ohmori K, *et al.* Histamine H1 receptor antagonist blocks histamine-induced proinflammatory cytokine production through inhibition of Ca2+-dependent protein kinase C, Raf/MEK/ERK and IKK/I kappa B/NF-kappa B signal cascades. Biochem Pharmacol 2005; 69:433–449.

55 Shiohara T, Hayakawa J, Mizukawa Y. Animal models for atopic dermatitis: are they relevant to human disease? J Dermatol Sci 2004; 36:1–9.

56 Man MQ, Hatano Y, Lee SH, *et al.* Characterization of a hapten-induced, murine model with multiple features of atopic dermatitis: structural, immunologic, and biochemical changes following single versus multiple oxazolone challenges. J Invest Dermatol 2008; 128:79–86.

57 Tamura T, Amano T, Ohmori K, *et al.* The effects of olopatadine hydrochloride on the number of scratching induced by repeated application of oxazolone in mice. Eur J Pharmacol 2005; 524:149–154.

58 • Murota H, Kitaba S, Tani M, *et al.* Effects of nonsedative antihistamines on productivity of patients with pruritic skin diseases. Allergy 2010; 65:929–930.

This literature firstly revealed the discrepancy of effect of sedative antihistamines on pruritus and impaired daily activity in dermatoses with pruritus.

59 • Murota H, Kitaba S, Tani M, *et al.* Impact of sedative and nonsedative antihistamines on the impaired productivity and quality of life in patients with pruritic skin diseases. Allergol Int 2010; 59:345–354.

This literature firstly revealed the discrepancy of effect of sedative antihistamines on pruritus and impaired daily activity in atopic dermatitis.

60 Thompson AK, Finn AF, Schoenwetter WF. Effect of 60 mg twice-daily fexofenadine HCl on quality of life, work and classroom productivity, and regular activity in patients with chronic idiopathic urticaria. J Am Acad Dermatol 2000; 43:24–30.

61 •• Church MK, Maurer M, Simons FE, *et al.* Risk of first-generation H(1)-antihistamines: a GA(2)LEN position paper. Allergy 2010; 65:459–466.

This is well organized position paper, which compiles the previous knowledge for adverse effect of first-generation antihistamines.

62 Parmentier R, Ohtsu H, Djebbara-Hannas Z, *et al.* Anatomical, physiological, and pharmacological characteristics of histidine decarboxylase knock-out mice: evidence for the role of brain histamine in behavioral and sleep-wake control. J Neurosci 2002; 22:7695–7711.

63 Lin JS. Brain structures and mechanisms involved in the control of cortical activation and wakefulness, with emphasis on the posterior hypothalamus and histaminergic neurons. Sleep Med Rev 2000; 4:471–503.

64 •• Van Ruitenbeek P, Vermeeren A, Riedel WJ. Cognitive domains affected by histamine H(1)-antagonism in humans: a literature review. Brain Res Rev 2010; 64:263–282.

This review article assessed the function of histamine H1-antagonism within cognitive domains based on the recent literatures.

65 Schwartz JC, Arrang JM, Garbarg M, *et al.* Histaminergic transmission in the mammalian brain. Physiol Rev 1991; 71:1–51.

66 Lin JS, Sakai K, Jouvet M. Evidence for histaminergic arousal mechanisms in the hypothalamus of cat. Neuropharmacology 1988; 27:111–122.

67 Shamsi Z, Hindmarch I. Sedation and antihistamines: a review of inter-drug differences using proportional impairment ratios. Hum Psychopharmacol 2000; 15:S3–S30.

68 Yanai K, Tashiro M. The physiological and pathophysiological roles of neuronal histamine: an insight from human positron emission tomography studies. Pharmacol Ther 2007; 113:1–15.

69 • Zhang D, Tashiro M, Shibuya K, *et al.* Next-day residual sedative effect after nighttime administration of an over-the-counter antihistamine sleep aid, diphenhydramine, measured by positron emission tomography. J Clin Psychopharmacol 2010; 30:694–701.

This literature firstly confirmed the hangover effect of nighttime administration of sedative antihistamine using imaging method.

70 Okamura N, Yanai K, Higuchi M, *et al.* Functional neuroimaging of cognition impaired by a classical antihistamine, d-chlorpheniramine. Br J Pharmacol 2000; 129:115–123.

71 Masaki T, Chiba S, Yasuda T, *et al.* Involvement of hypothalamic histamine H1 receptor in the regulation of feeding rhythm and obesity. Diabetes 2004; 53:2250–2260.

72 Fulop AK, Foldes A, Buzas E, *et al.* Hyperleptinemia, visceral adiposity, and decreased glucose tolerance in mice with a targeted disruption of the histidine decarboxylase gene. Endocrinology 2003; 144:4306–4314.

73 Ratliff JC, Barber JA, Palmese LB, *et al.* Association of prescription
• H1 antihistamine use with obesity: results from the National Health and Nutrition Examination Survey. Obesity (Silver Spring) 2010; 18:2398–2400.

This literature firstly showed the verification outcome of possible inolvement of taking antihistamines to obesity.

74 Murota H, Takahashi A, Nishioka M, *et al.* Showering reduces atopic dermatitis in elementary school students. Eur J Dermatol 2010; 20:410–411.

75 Wollenberg A, Rawer HC, Schauber J. Innate Immunity in Atopic Dermatitis. Clin Rev Allergy Immunol 2010.

76 Ertam I, Biyikli SE, Yazkan FA, *et al.* The frequency of nasal carriage in chronic urticaria patients. J Eur Acad Dermatol Venereol 2007; 21:777–780.

77 St Peter SD, Sharp SW, Ostlie DJ. Influence of histamine receptor antagonists on the outcome of perforated appendicitis: analysis from a prospective trial. Arch Surg 2010; 145:143–146.

78 Metz M, Doyle E, Bindslev-Jensen C, *et al.* Effects of antihistamines on innate
•• immune responses to severe bacterial infection in mice. Int Arch Allergy Immunol 2011; 155:355–360.

This literature revealed the effect of antihistamines on innate immune responses clearly using animal model.

JBC Papers in Press. Published on June 22, 2011 as Manuscript M111.220376
The latest version is at http://www.jbc.org/cgi/doi/10.1074/jbc.M111.220376

ENHANCED EPITHELIAL-MESENCHYMAL TRANSITION-LIKE PHENOTYPE IN *N*-ACETYLGLUCOSAMINYLTRANSFERASE V TRANSGENIC MOUSE SKIN PROMOTES WOUND HEALING

Mika Terao[1,2]*, Akiko Ishikawa[1]*, Susumu Nakahara[3], Akihiro Kimura[1], Arisa Kato[1], Kenta Moriwaki[1], Yoshihiro Kamada[1], Hiroyuki Murota[2], Naoyuki Taniguchi[3], Ichiro Katayama[2], Eiji Miyoshi[1,3]

From Department of Molecular Biochemistry and Clinical Investigation[1], Department of Dermatology[2], Department of Biochemistry[3], Osaka University Graduate School of Medicine.

*These authors equally contribute to this work.

Running head: EMT-like phenotype in GnT-V Tg mice

Address correspondence to: Department of Molecular Biochemistry and Clinical Investigation, 1-7, Yamada-oka, Suita 565-0871, Japan. Fax: +81-6-6879-2590; E-mail: emiyoshi@sahs.med.osaka-u.ac.jp

***N*-Acetylglucosaminyltransferase-V (GnT-V) catalyzes the β1,6 branching of *N*-acetylglucosamine on *N*-glycans. GnT-V expression is elevated during malignant transformation in various types of cancer; however, the mechanism by which GnT-V promotes cancer progression is unclear. To characterize the biological significance of GnT-V, we established GnT-V transgenic (Tg) mice, in which GnT-V is regulated by a β-actin promoter. No spontaneous cancer was detected in any organs of the GnT-V Tg mice. However, GnT-V expression was upregulated in GnT-V Tg mouse skin, and cultured keratinocytes derived from these mice showed enhanced migration, which was associated with changes in E-cadherin localization, and epithelial-mesenchymal transition (EMT). Further, EMT–associated factors snail, twist, and, N-cadherin were upregulated, and cutaneous wound healing was accelerated *in vivo*. We further investigated the detailed mechanisms of EMT by assessing epidermal growth factor (EGF) signaling and found upregulated EGF receptor signaling in GnT-V Tg mouse keratinocytes. These findings indicate that GnT-V overexpression promotes EMT and keratinocyte migration in part through enhanced EGF receptor signaling.**

Oligosaccharide structure changes are detected following birth, differentiation, and carcinogenesis (1), and these changes are regulated by glycosyltransferases. In particular, *N*- acetylglucosaminyltransferase V (GnT-V) plays an important role in carcinogenesis and tumor metastasis (2). To characterize the detailed molecular mechanisms underlying GnT-V－related tumor metastasis, we and other groups succeeded in purifying and cloning GnT-V (3-5). In addition, we developed a sugar remodeling system of cancer cells and demonstrated the biological function of GnT-V in tumor metastasis through biochemical analysis of its target glycoproteins (6). Dennis et al. reported that mammary tumor growth and metastases induced by the polyomavirus middle T oncogene was considerably less in GnT-V deficient mice than in littermate control mice. (7). Cancer cells established from GnT-V–deficient mice showed lower cell growth and intracellular signaling than control mice because of aberrant glycosylation of growth factor receptors (8). Dennis et al. also reported that sugar metabolism is critical to control the formation of β1,6 *N*-acetylglucosamine (GlcNAc), a product of GnT-V (9). In contrast, GnT-V is involved in negative regulation of T cell activation, leading to suppress autoimmunity reaction (10). Recently, Mkhikian *et al.* reported that genetic changes in glycosylation status for suppressing *N*-glycan branching are concerned with the incidence of Multiple Sclerosis (11). Our groups have studied biological functions of adhesion molecules such as cadherin and integrins in terms of N-glycan branching mediated by GnT-V and have found that GnT-V inhibits cell-cell/cell-matrix adhesion and promotes migration of cancer cells (12).

Although GnT-V is known to be upregulated in the early phase of carcinogenesis in many cancers (13), it is unclear whether

Copyright 2011 by The American Society for Biochemistry and Molecular Biology, Inc.

Downloaded from www.jbc.org at OSAKA UNIVERSITY, on July 25, 2011

GnT-V regulates the late phase of cancer progression. In the case of colon cancer, GnT-V expression is associated with poor prognosis (14); in contrast, low GnT-V levels are linked to poor prognosis in lung and bladder carcinomas (15,16). These reports suggest that the role of GnT-V in cancer progression is organ-specific. Thus, we developed the GnT-V Tg mouse model to characterize the biological effects of GnT-V overexpression in normal tissues.

High GnT-V expression was observed in the skin of GnT-V Tg mice, and an epithelial-mesenchymal transition (EMT)-like phenotype was observed in cultured keratinocytes derived from these mice. EMT, which is characterized by the loss of epithelial adhesion and gain of mesenchymal features, is a fundamental biological process of embryonic development and cancer invasion/metastasis (17). In adults, EMT, which is driven by the cytokine bath generated by tissue injury, mediates the production of fibroblasts during inflammation and wound healing (18-20). Re-epithelialization in wound healing involves the motility or migration of epithelial cells, and the migrating epithelial cells in wound margins acquire mesenchymal features and follow early stages of EMT (18).

In the present study, we analyzed the EMT-like phenotypes of keratinocytes from GnT-V Tg mice and found that enhanced keratinocyte motility and cutaneous wound healing were mediated in part by aberrant epidermal growth factor (EGF) receptor signaling.

Experimental Procedures

GnT-V expression vector- We used the expression vector pCAGGS, which contains a human β-actin promoter fused to a human β-globin gene fragment and polyadenylation signals (21). A construct containing the full-length GnT-V cDNA was constructed (5), as shown in Fig.1.

Establishment of transgenic mice- Bromodomain factor 1 (BDF1) mice used in this study were purchased from SLC Co. (Shizuoka, Japan) and maintained under specific-pathogen-free conditions. After microinjection of *Sal*I-linearized Mgat5 expression vector into the pronuclei of BDF1-derived zygotes, the zygotes were introduced into the ampullae of pseudopregnant BDF1 mice, which gave birth to litters of 10 to 14 mice 21 days later. Newborn mice were genotyped by Southern blot analysis of *BamH*I-digested genomic DNA isolated from tail tissues, using a DNA fragment containing the Mgat5 gene coding region as a probe. Transgene-positive F_1 mice were backcrossed to wild- type BDF1 mice to generate stable lines. Subsequently, transgene-positive mice were identified by PCR using genomic DNA from mice as templates and confirmed by Southern blot analysis with the probe described above. PCR conditions were: 95°C for 1 min followed by 37 cycles of denaturation at 94°C for 30 sec, annealing at 54°C for 30 sec, and extension at 72°C for 50 sec. Human Mgat5 primers were used: 5′-GTGCTGGTTGTTGTGCTGTC-3′ (sense) and 5′-CTTGATTGCTTGGATCC-3′ (anti-sense) (19). Transgene-negative littermates were used as control mice. All mice were maintained in a specific pathogen-free facility at Osaka University. The Institutional Animal Care and Use Committee at Osaka University approved all procedures.

Cell culture- Mouse keratinocytes and were isolated and cultured as previously described (22). Full-thickness tail skin harvested from 12-week-old mice was treated with 4 mg/ml of dispase (Gibco, Invitrogen Paisley, UK) for 1 h at 37°C. The epidermis was then peeled from the dermis and trypsinized to prepare single-cell suspensions. Cells were incubated in human keratinocyte serum-free medium (DS Pharma Biomedical, Osaka, Japan) for 6 to 12 h at 37°C in 5% CO_2 to allow the cells to adhere to culture dishes pre-coated with type-1 collagen (Asahi Techno Glass, Funabashi, Japan). Non-adherent cells were washed with phosphate-buffered saline twice and then cultured for 2 to 3 days in human keratinocyte serum-free medium before use in experiments.

Assay of enzyme activities- Assay of GnT-V activity was carried out according to previous report, with slight modifications (23). Assay employed (pH 6.25), 250 mM Mes buffer, containing 400 mM UDP-GlcNAc, 20 mM EDTA, 400 mM *N*-acetylglucosamine, 2 mg/ml BSA, and 1.0% Triton X-100. First, 0.5 μl of 100 mM substrate was added to 6.5 μl of this solution. Following this, 3.5 μl of enzyme solution were added and the mixture was incubated at 37°C for 4 h. The enzyme reactions were stopped by heating at 100°C for 5 min. The samples were added with 25 μl water and

Downloaded from www.jbc.org at OSAKA UNIVERSITY, on July 25, 2011

centrifuge at 15,000 rpm for 15 min. Supernatants were applied to a TSKgel ODS-80TM column (4.6 ×150 mm). Elution was performed at 55°C with a 0.1 M acetate buffer (pH 4.0) containing 1% *n*-butanol at a flow rate of 1.0 ml/min. The specific activity of GnT-V is expressed as pmol of *N*-acetylglucosamine transferred / h / mg of protein.

Immunofluorescence staining of keratinocytes- Mouse keratinocytes were isolated as described above, seeded into dishes pre-coated with type-1 collagen (5×10^5 cells/ml), and grown to confluence. Cells were then fixed with 4% paraformaldehyde and permeabilized with 0.5% Triton X (for α-smooth muscle actin). The cells were then incubated with the primary antibodies rat anti-E-Cadherin (1:500 dilution; Sigma-Aldrich, St. Louis, MO, USA), mouse anti-α-smooth muscle actin (SMA, 1:300 dilution; DakoCytomation, Carpinteria, CA, USA), rabbit anti-cytokeratin 5 (1:1000 dilution; Covance, Emeryville, CA, USA), followed by the secondary antibody (anti-rabbit Alexa Fluor 555 or anti-mouse Alexa Fluor 488; Invitrogen). The cells were visualized using a Keyence Biozero confocal microscope.

Immunohistochemistry and immunofluorescence staining of skin sections- Mouse dorsal skin samples were fixed in 10% formaldehyde for 24 h followed by paraffin embedding and microtome sectioning. Slides were then stained with hematoxylin and eosin (H&E). For immunohistochemical analysis, sections were hydrated by passage through xylene and graded ethanols. After antigen retrieval for 10 min at 95°C in citrate buffer (pH 6) the slides were blocked with serum-free protein block (DakoCytomation) for 15 min, and then incubated overnight at 4°C with the primary antibody mouse anti-E-cadherin (1:100 dilution, R&D Systems, Minneapolis, MN, USA). After washing with Tris-buffered saline (TBS) containing 0.05% Triton-X100, the slides were developed with the DAKO LSAP+System-AP (DakoCytomation), Dako ChemMate Envision kit/HRP(DAB) and then counterstained with hematoxylin. Rabbit and mouse IgG were used as the isotype controls.

RNA isolation and quantitative real time polymerase chain reaction (rtPCR)- Total RNA was isolated from mouse epidermis and keratinocytes using the SV Total RNA Isolation System (Promega, Madison, WI) and reverse-transcribed into cDNA. Expression of E-cadherin, α-SMA, N-cadherin, snail, and twist were determined using Power SYBR green PCR Master Mix (Applied Biosystems, Foster City, CA) according to the manufacturer's protocol. Glyceraldehyde-3-phosphate dehydrogenase (GAPDH) was used to normalize target gene expression. Sequence-specific primers were designed as follows: E-cadherin, sense 5′-ggctggctgaaagtgacaca-3′, antisense 5′-acggcatgagaatagaggatgtact-3′; α-SMA, sense 5′-tctctatgctaacaacgtcctgtca-3′, antisense 5′-ccaccgatccagacagagtactt-3′; N-cadherin, sense 5′-gagcctatgaaggaaccacatga-3′; snail, sense 5′-aacatgccgcgctcctt-3′, antisense 5′-ggtcgtagggctgctggaa-3′; twist, sense 5′-ccggagagacctagatgtcattgtt-3′, antisense 5′-agttattccagctccagagtctctag-3′; GAPDH, sense 5′-tgtcatcatacttggcaggtttct-3′, antisense 5′-catggccttccgtgttccta-3′. PCR amplification consisted of 40 cycles of denaturing at 92°C for 15 seconds and annealing at 60°C for 60 seconds on an ABI 7000 Prism (Applied Biosystems).

Western blot analysis- Cell samples were solubilized at 4°C in TNE buffer consisting of 10 mM Tris-HCl (pH 7.8), 1% Nonidet P-40, 0.15 M NaCl, 1 mM EDTA, and protease inhibitor cocktail (Wako, Osaka, Japan). For *in vivo* samples, skin specimens were crushed in liquid nitrogen and solubilized at 4°C in TNE buffer. Same amount of proteins (10–30 μg depending on each experiment) were separated by SDS-PAGE and transferred onto polyvinylidene fluoride membranes (Bio-Rad, Hercules, CA, USA). Non-specific protein binding was blocked by incubation in 5% w/v non-fat milk powder in TBS-T (50 mM Tris-HCl [pH 7.6], 150 mM NaCl, and 0.1% v/v Tween-20). The membranes were then incubated with rat anti-E-cadherin antibody (Sigma-Aldrich), rabbit anti-cytokeratin 5 antibody (Covance), anti-α-SMA antibody (DakoCytomation), or mouse anti-GnT-V antibody 24D11 (provided from Fujirebio, Hachioji, Japan), each at 1:1000 dilution overnight at 4°C, or with mouse monoclonal anti-β-actin (Sigma-Aldrich) at 1:5000 for 30 min at room temperature. The membranes were then washed three times in TBS-T (5 min each wash). Finally, the membranes were incubated with horseradish peroxidase (HRP)-conjugated anti-rabbit, anti-mouse or anti-rat antibodies (1:10,000 dilution) for 60 min

Downloaded from www.jbc.org at OSAKA UNIVERSITY, on July 25, 2011

at room temperature. Protein bands were detected by chemiluminescence using the ECL Plus kit (GE Healthcare, Buckinghamshire, UK). Band intensity was quantified with ImageJ software (National Institutes of Health, Bethesda, MD, USA).

Lectin blotting and lectin precipitation- For lectin blotting, membranes were blocked with 3% bovine serum albumin in TBS-T, followed by incubation with 10 μg/ml biotinylated phytohemagglutinin-L_4 (L_4-PHA) lectin (J-Oil Mills, Tokyo, Japan). Reactive bands were detected using the ECL Plus kit (GE Healthcare). For lectin-precipitation, skin protein samples (2.7 mg) were incubated with 50 μl L_4-PHA lectin agarose (J-Oil Mills) for 2 h at 4°C and then centrifuged at 2000 rpm for 2 min. The lectin precipitates were washed two times with TNE buffer, and the bound proteins were boiled in 50 μl 2× SDS sample buffer, eluted, resolved by 6% SDS-PAGE, and finally transferred onto nitrocellulose membranes (GE Healthcare), as previously described (24). The membrane was incubated with rabbit anti-EGF-R antibody (1:500 dilution; Cell Signaling Technology, Beverly, MA, USA) and probed with HRP-conjugated anti-rabbit, and proteins were detected by chemiluminescence.

In vitro migration assay- Mouse keratinocytes were isolated as previously described, seeded into dishes pre-coated with type-1 collagen (1.3×10^6 cells/3.5cm dish) and grown to confluence. After serum starvation for 24 h, they were treated with 10 μg/ml mitomycin C for 30 min to inhibit proliferation. A cell-free area was introduced by scraping the monolayer with a pipette tip. Cell migration to the cell-free area was evaluated in the presence or absence of EGF (10 ng/ml; R&D Systems) or the EGF-R inhibitor AG1478 (10 nM; LC Laboratories, Woburn, MA, USA)

Wound healing assay- BDF1 GnT-V Tg mice were back-crossed to Hr-/Kud mice more than seven times. Full-thickness 8-mm punch biopsies were performed on the backs of 16-week-old male Hr-/Kud mice (n=5) and GnT-V Tg mice (n=8). The wound areas were analyzed on days, 0, 2, 4, 6, 8, 10, 12, and 14 after the biopsy was performed.

Statistical Analysis- The results are representative of at least three independent experiments. *p* values were calculated using a two-sided unpaired-Student's-*t* test.

RESULTS

Establishment of transgenic mouse line expressing GnT-V. The Mgat5 (GnT-V)–expressing construct used to generate mouse lines is shown in Fig. 1A. Expression of GnT-V protein assessed by Western blot was increased in many tissues of the transgenic mice, including skin, brain, pancreas, kidney, and liver (Fig. 1B). GnT-V activities evaluated by HPLC were almost consistent with the data of Western blot (Fig. 1C). To evaluate the oligosaccharide structures of skin glycoproteins, skin homogenates were assessed by lectin blot analysis with L_4-PHA, which is known to react preferentially with β1,6 GlcNAc (25). Skin homogenates from GnT-V Tg mice showed higher reactivity to L_4-PHA than those of wild-type mice (Fig. 1D). H&E staining of GnT-V Tg mouse skin did not reveal differences from the wild-type controls (Fig. 1E).

Enhanced migration of GnT-V Tg mouse keratinocytes. Although GnT-V expression is upregulated in various cancers, GnT-V overexpression did not result in any spontaneous cancers in GnT-V Tg mice within the first year. However, the healing of minor wounds of the back skin made by fighting was markedly accelerated in GnT-V Tg mice compared with wild-type controls. We speculated that re-epithelialization might be enhanced in GnT-V Tg mice and therefore evaluated *in vitro* migration of GnT-V Tg mouse keratinocytes. The number of cells that migrated to a cell-free area (created by scraping the cell culture monolayer with a pipette tip) was significantly higher in GnT-V Tg keratinocytes than controls (Fig. 2A-C). The cells of migrating edge showed spindle shape in GnT-V Tg mouse keratinocytes compared with wild-type control keratinocytes. The spindle-shaped cells expressed keratin 5, suggesting that it had a character of keratinocytes (Fig. 2D). A ratio of Ki-67 positive cells was not different between wild-type and GnT-V Tg mouse keratinocytes, indicating that cell proliferation did not significantly differ between GnT-V Tg and wild-type keratinocytes (Fig. 2E, F). In addition to enhanced cell migration, evaluation of primary keratinocytes in cultures derived from GnT-V Tg epidermis showed decreased expression of E-cadherin (Fig. 3A). The number of cells expressing N-cadherin was higher in

Downloaded from www.jbc.org at OSAKA UNIVERSITY, on July 25, 2011

GnT-V Tg keratinocytes, compared to that of wild-type keratinocytes (Fig. 3B). Further, the number of α-SMA expressing cells was also increased in GnT-V Tg keratinocytes (Fig. 3C), and cells expressing both K5 and α-SMA, epidermal and mesenchymal markers were also observed (Fig. 3D). Decreases in E-cadherin were confirmed by Western blot (Figure 3E). However, we were not able to detect N-cadherin by Western blot (data not shown).

EMT-like features are induced in GnT-V Tg mouse skin tissue. Delocalization of E-cadherin, acquisition of mesenchymal characteristics, and increased cell mobility are features of the early stage of EMT (26). We evaluated these EMT features in GnT-V Tg mouse keratinocytes by first determining EMT-related gene expression by real-time PCR analysis. Expression of the EMT-related transcription factors snail and twist were increased in GnT-V Tg mouse keratinocytes (Fig. 4). The switch from E-cadherin to N-cadherin results in loss of the epithelial phenotype and acquisition of the mesenchymal phenotype (27). We found that mRNA levels of N-cadherin was elevated in GnT-V Tg keratinocytes, although E-cadherin was not significantly reduced (Fig. 4). Taken together, these data demonstrate that EMT-like features were induced in GnT-V Tg mouse keratinocytes and may contribute to the enhanced migration of GnT-V Tg keratinocytes.

Aberrant glycosylation of EGF-R enhances its signaling in GnT-V Tg mouse keratinocytes. The autocrine/paracrine signaling of cytokines, such as EGF, transforming growth factor-beta (TGF-β), and tumor necrosis factor-alpha (TNF-α), regulate EMT morphologic phases in keratinocytes (18,28,29). EGF family members are primary growth factors involved in re-epithelialization during cutaneous wound healing (30,31). High levels of β1,6 GlcNAc branching in EGF-Rs of GnT-V Tg mouse skin were inferred from the finding that EGF-R levels of GnT-V Tg mouse skin precipitated with L_4-PHA lectin were significantly higher than those of controls (Fig. 5A). Glycosylation of EGF-R modulates EGF-R signaling (32); therefore, we evaluated EGF-R signaling by determining the level of ERK phosphorylation induced by EGF (10 ng/ml). As expected, prolonged phosphorylation of ERK was observed after EGF treatment of GnT-V Tg keratinocytes (Fig. 5B), and migration was enhanced by EGF in these cells (Fig. 5C). These findings suggest that increased β1,6 GlcNAc branching on EGF-R induced by GnT-V overexpression modulates EGF-R signaling, thereby altering EMT features in the skin.

EGF-R inhibitor attenuates migration of GnT-V Tg keratinocytes. To confirm the significance of EGF-R signaling in the EMT-like features of GnT-V Tg mice, we evaluated the effects of the EGF-R inhibitor AG1478 on keratinocyte migration *in vitro*. We found that AG1478 attenuated migration in GnT-V Tg keratinocytes (Fig. 5D). These results showed that EGF-R signaling was involved in the enhanced migration of GnT-V Tg keratinocytes.

Abberant glycosylation was increased on E-cadherin in GnT-V Tg mouse keratinocytes
We next examined whether or not glycosylation of E-cadherin was altered in GnT-V Tg mouse keratinocytes. Cell lysate of wild-type and GnT-V Tg mouse keratinocytes were immunoprecipitated with anti-E-cadherin antibodies and the binding of immunoprecipitants to L_4-PHA were evaluated by lectin blot analysis. While levels of total immunoprecipitated E-cadherin were lower in GnT-V Tg mouse keratinocytes, almost the same intensity of bands binding to L_4PHA was observed between GnT-V Tg and wild-type mouse keratinocytes, suggesting that aberrant glycosylation on E-cadherin was increased in GnT-V Tg mouse keratinocytes (Fig. 5E).

Wound healing was accelerated in GnT-V Tg mice. To evaluate EMT-like phenotype and the enhanced migration of GnT-V Tg mouse keratinocytes *in vivo*, we performed a cutaneous wound healing assay using 8-mm round wounds on the backs of GnT-V Tg and control mice. The wound areas in GnT-V Tg mice were significantly lower than controls on days 2, 4, 6, 8, and 10 (Fig. 6A, B); mean wound closure was 16.0±1.81 days in control mice and 14.4±1.91 days in GnT-V Tg mice (Fig. 6C). Notably, re-epithelialization was more rapid in GnT-V Tg mice (Fig. 6D). These results demonstrate that re-epithelialization of cutaneous wounds was enhanced in GnT-V Tg mice due to the enhanced EMT-like phenotype.

DISCUSSION

Downloaded from www.jbc.org at OSAKA UNIVERSITY, on July 25, 2011

Recently, EMT has become a focus of cancer research as molecular and morphologic features of EMT are found to correlate with poor histological differentiation, loss of tissue integrity, and metastasis (33). Characteristics of EMT *in vitro* include increased expression of mesenchymal factors (collagen I and vimentin), cadherin switch, loss of epithelial markers, spindle-shape morphology, increased migratory capacity, and resistance to apoptotic stimuli (17).

In the present study, we detected EMT-like features in the skin of GnT-V Tg mice, including expression of mesenchymal factors, spindle-shape morphology, and increased migration (Fig. 2). Epithelial wound closure, dermal repair, and angiogenesis are steps in the repair of cutaneous wounds (31,34). Motility and migration of epithelial cells, which are key steps in re-epithelialization, follow the early stage phenomena of EMT (18,35). Cutaneous wound healing *in vivo* and keratinocyte mobility *in vitro* was accelerated in GnT-V Tg mice because GnT-V overexpression promoted EMT in the epidermis of transgenic mice (Fig. 4). This result was consistent with data of previous *in vitro* study that overexpresion of GnT-V in Mv1Lu cells enhanced the migration to scratch wound (36).

GnT-V expression is associated with poor prognosis in breast cancer (37), colon cancer (14), and endometrial cancer (38). Consistent with these studies, we found that GnT-V was upregulated in some cases of poorly differentiated invasive squamous skin carcinoma (manuscript in preparation). These results suggest that GnT-V–associated EMT is involved in the progression of these carcinomas.

EMT features in cutaneous wound healing differ from the features of cancer metastasis because epithelial cells involved in wound healing that acquire mobility and mesenchymal phenotypes return to the epithelial phenotype. In GnT-V Tg mice, the early phase phenomena of EMT and enhanced re-epithelialization were observed but spontaneous carcinoma did not occur during the 1-year study period, suggesting that GnT-V overexpression in the skin is not sufficient to induce cancer development. Gene mutation(s) and oncogene activation appear to be required for spontaneous carcinogenesis; thus, GnT-V overexpression in pre-malignant conditions may produce results that differ from those of the present study. Experimental carcinogenesis in our GnT-V Tg model may be useful to answer this problem in the future.

EGF-R signaling essential for keratinocyte migration and proliferation in EMT is predominantly regulated by autocrine EGF-R activation (39,40). EGF-R mediated proliferation and migration of keratinocytes also appears to be crucial in wound healing; keratinocytes play a central role in wound repair as a source of growth factors (26,39). Previous studies reported that GnT-V–deficient mammary tumor cells showed reduced EGF-R signaling through decreased galectin-3 binding to polylactosamine structures and rapid internalization of the receptors from the cell surface (41). Mammary tumor cells from GnT-V–knockout mice are insensitive to EGF, fibroblast growth factor, and TGF-β (8). Downregulation of β1,6 GlcNAc branching by GnT-III overexpression also decreased EGF-R signaling (26). As EGF-R signaling was increased in GnT-V Tg mouse keratinocytes, we hypothesized that overexpression of GnT-V promotes an EMT-like phenotype in wound healing in part by modulated EGF-R signaling.

We also assume that modification of E-cadherin N-glycans by GnT-V also played a role in keratinocyte migration as post-transcriptional modification of E-cadherin by GnT-V is reported to de-localize E-cadherin to cytoplasm (42,43). Since expression of E-cadherin was not altered at mRNA level but was decreased at protein level in GnT-V Tg mouse keratinocytes, we consider that increase in aberrant glycosylation of E-cadherin might down-regulate the expression of E-cadherin at protein level. In our previous reports, reverse phenomenon was observed in mouse melanoma cells transfected with N-acetylglucosaminyltransferase III (GnT-III) gene (44). Since GnT-III suppresses a reaction of GnT-V and prolongs half life of E-cadherin, the instability of E-cadherin modulated by GnT-V in the present study seems to be compatible with our previous data. Modulation of her-2-mediated signaling pathways by GnT-V might also affect GnT-V Tg mouse keratinocytes as it is known to regulate the proportion of tumor initiating cells (45).

In conclusion, we found EMT features in GnT-V Tg mice that contributed to keratinocyte mobility and cutaneous wound healing were

Downloaded from www.jbc.org at OSAKA UNIVERSITY, on July 25, 2011

mediated in part by upregulated EGF receptor signaling. These findings suggest that GnT-V overexpression in keratinocytes induces the early phase of malignant transformation. Future experiments involving carcinogen induction or mating GnT-V Tg mice with other carcinogenic mice may be useful to test this hypothesis.

REFERENCES

1. Rademacher, T. W., Parekh, R. B., and Dwek, R. A. (1988) *Annu Rev Biochem* **57**, 785-838
2. Dennis, J. W., Granovsky, M., and Warren, C. E. (1999) *Biochim Biophys Acta* **1473**, 21-34
3. Shoreibah, M., Perng, G. S., Adler, B., Weinstein, J., Basu, R., Cupples, R., Wen, D., Browne, J. K., Buckhaults, P., Fregien, N., and Pierce, M. (1993) *J Biol Chem* **268**, 15381-15385
4. Shoreibah, M. G., Hindsgaul, O., and Pierce, M. (1992) *J Biol Chem* **267**, 2920-2927
5. Saito, H., Nishikawa, A., Gu, J., Ihara, Y., Soejima, H., Wada, Y., Sekiya, C., Niikawa, N., and Taniguchi, N. (1994) *Biochem Biophys Res Commun* **198**, 318-327
6. Taniguchi, N., Ihara, S., Saito, T., Miyoshi, E., Ikeda, Y., and Honke, K. (2001) *Glycoconj J* **18**, 859-865
7. Granovsky, M., Fata, J., Pawling, J., Muller, W. J., Khokha, R., and Dennis, J. W. (2000) *Nat Med* **6**, 306-312
8. Partridge, E. A., Le Roy, C., Di Guglielmo, G. M., Pawling, J., Cheung, P., Granovsky, M., Nabi, I. R., Wrana, J. L., and Dennis, J. W. (2004) *Science* **306**, 120-124
9. Dennis, J. W., Nabi, I. R., and Demetriou, M. (2009) *Cell* **139**, 1229-1241
10. Demetriou, M., Granovsky, M., Quaggin, S., and Dennis, J. W. (2001) *Nature* **409**, 733-739
11. Mkhikian, H., Grigorian, A., Li, C. F., Chen, H. L., Newton, B., Zhou, R. W., Beeton, C., Torossian, S., Tatarian, G. G., Lee, S. U., Lau, K., Walker, E., Siminovitch, K. A., Chandy, K. G., Yu, Z., Dennis, J. W., and Demetriou, M. (2011) *Nat Commun* **2**, 334
12. Isaji, T., Kariya, Y., Xu, Q., Fukuda, T., Taniguchi, N., and Gu, J. (2010) *Methods Enzymol* **480**, 445-459
13. Miyoshi, E., Nishikawa, A., Ihara, Y., Gu, J., Sugiyama, T., Hayashi, N., Fusamoto, H., Kamada, T., and Taniguchi, N. (1993) *Cancer Res* **53**, 3899-3902
14. Murata, K., Miyoshi, E., Kameyama, M., Ishikawa, O., Kabuto, T., Sasaki, Y., Hiratsuka, M., Ohigashi, H., Ishiguro, S., Ito, S., Honda, H., Takemura, F., Taniguchi, N., and Imaoka, S. (2000) *Clin Cancer Res* **6**, 1772-1777
15. Dosaka-Akita, H., Miyoshi, E., Suzuki, O., Itoh, T., Katoh, H., and Taniguchi, N. (2004) *Clin Cancer Res* **10**, 1773-1779
16. Ishimura, H., Takahashi, T., Nakagawa, H., Nishimura, S., Arai, Y., Horikawa, Y.,

Downloaded from www.jbc.org at OSAKA UNIVERSITY, on July 25, 2011

Habuchi, T., Miyoshi, E., Kyan, A., Hagisawa, S., and Ohyama, C. (2006) *Clin Cancer Res* **12**, 2506-2511

17. Zeisberg, M., and Neilson, E. G. (2009) *J Clin Invest* **119**, 1429-1437
18. Yan, C., Grimm, W. A., Garner, W. L., Qin, L., Travis, T., Tan, N., and Han, Y. P. (2010) *Am J Pathol* **176**, 2247-2258
19. Kalluri, R., and Neilson, E. G. (2003) *J Clin Invest* **112**, 1776-1784
20. Desmouliere, A. (1995) *Cell Biol Int* **19**, 471-476
21. Niwa, H., Yamamura, K., and Miyazaki, J. (1991) *Gene* **108**, 193-199
22. Terao, M., Murota, H., Kitaba, S., and Katayama, I. (2010) *Exp Dermatol* **19**, 38-43
23. Nishikawa, A., Gu, J., Fujii, S., and Taniguchi, N. (1990) *Biochim Biophys Acta* **1035**, 313-318
24. Ihara, S., Miyoshi, E., Ko, J. H., Murata, K., Nakahara, S., Honke, K., Dickson, R. B., Lin, C. Y., and Taniguchi, N. (2002) *J Biol Chem* **277**, 16960-16967
25. Cummings, R. D., and Kornfeld, S. (1982) *J Biol Chem* **257**, 11230-11234
26. Pastore, S., Mascia, F., Mariani, V., and Girolomoni, G. (2008) *J Invest Dermatol* **128**, 1365-1374
27. Katoh, Y., and Katoh, M. (2008) *Int J Mol Med* **22**, 271-275
28. Wilkins-Port, C. E., and Higgins, P. J. (2007) *Cells Tissues Organs* **185**, 116-122
29. Freytag, J., Wilkins-Port, C. E., Higgins, C. E., Higgins, S. P., Samarakoon, R., and Higgins, P. J. (2010) *J Invest Dermatol* **130**, 2179-2190
30. Hardwicke, J., Schmaljohann, D., Boyce, D., and Thomas, D. (2008) *Surgeon* **6**, 172-177
31. Shirakata, Y., Kimura, R., Nanba, D., Iwamoto, R., Tokumaru, S., Morimoto, C., Yokota, K., Nakamura, M., Sayama, K., Mekada, E., Higashiyama, S., and Hashimoto, K. (2005) *J Cell Sci* **118**, 2363-2370
32. Sato, Y., Takahashi, M., Shibukawa, Y., Jain, S. K., Hamaoka, R., Miyagawa, J., Yaginuma, Y., Honke, K., Ishikawa, M., and Taniguchi, N. (2001) *J Biol Chem* **276**, 11956-11962
33. Christiansen, J. J., and Rajasekaran, A. K. (2006) *Cancer Res* **66**, 8319-8326
34. Werner, S., Krieg, T., and Smola, H. (2007) *J Invest Dermatol* **127**, 998-1008
35. Chen, J. D., Lapiere, J. C., Sauder, D. N., Peavey, C., and Woodley, D. T. (1995) *J Invest Dermatol* **104**, 729-733
36. Demetriou, M., Nabi, I. R., Coppolino, M., Dedhar, S., and Dennis, J. W. (1995) *J Cell Biol* **130**, 383-392
37. Dennis, J. W., and Laferte, S. (1989) *Cancer Res* **49**, 945-950
38. Yamamoto, E., Ino, K., Miyoshi, E., Shibata, K., Takahashi, N., Kajiyama, H., Nawa,

Downloaded from www.jbc.org at OSAKA UNIVERSITY, on July 25, 2011

A., Nomura, S., Nagasaka, T., and Kikkawa, F. (2007) *Br J Cancer* **97**, 1538-1544

39. Hudson, L. G., and McCawley, L. J. (1998) *Microsc Res Tech* **43**, 444-455
40. Stoll, S., Garner, W., and Elder, J. (1997) *J Clin Invest* **100**, 1271-1281
41. Lajoie, P., Partridge, E. A., Guay, G., Goetz, J. G., Pawling, J., Lagana, A., Joshi, B., Dennis, J. W., and Nabi, I. R. (2007) *J Cell Biol* **179**, 341-356
42. Pinho, S. S., Reis, C. A., Paredes, J., Magalhaes, A. M., Ferreira, A. C., Figueiredo, J., Xiaogang, W., Carneiro, F., Gartner, F., and Seruca, R. (2009) *Hum Mol Genet* **18**, 2599-2608
43. Pinho, S. S., Seruca, R., Gartner, F., Yamaguchi, Y., Gu, J., Taniguchi, N., and Reis, C. A. (2011) *Cell Mol Life Sci*
44. Yoshimura, M., Ihara, Y., Matsuzawa, Y., and Taniguchi, N. (1996) *J Biol Chem* **271**, 13811-13815
45. Guo, H. B., Johnson, H., Randolph, M., Nagy, T., Blalock, R., and Pierce, M. (2010) *Proc Natl Acad Sci U S A* **107**, 21116-21121

Downloaded from www.jbc.org at OSAKA UNIVERSITY, on July 25, 2011

ACKNOWLEDGEMENT

This study was performed by a grant from the Global COE program of Osaka University funded by the Ministry of Education, Culture, Sports, Science, and Technology of Japan, Grant-in-Aid for Young Scientists (B), No. 22791069, and a Grant-in-Aid for Scientific Research (A), No. 21249038, from the Japan Society for the Promotion of Science.

The abbreviations used are: GnT-V, *N*-Acetylglucosaminyltransferase-V; EMT, epithelial-mesenchymal transition; EGF, epidermal growth factor; BDF1, bromodomein factor 1.

FIGURE LEGENDS

Fig. 1. Establishment of GnT-V Tg mice. *(A)* Construct used to generate mouse lines expressing GnT-V (left). Transgene-positive mice were identified by PCR using genomic DNA from obtained from tails (right). *(B)* Expression of GnT-V in multiple organs as assessed by Western blot analysis. *(C)* The activity of GnT-V was assayed by our conventional methods using HPLC. *(D)* The extent of β1,6 GlcNAc branching, catalyzed by GnT-V, was assessed by L_4-PHA lectin blot analysis of skin tissue. *(E)* Histologic analysis of the tail skin of wild-type and GnT-V tg mice (H&E staining).

Fig. 2. Enhanced migration of GnT-V Tg mouse keratinocytes. Scrape-wounded, confluent keratinocyte monolayers of Wildt-type and Tg mice were incubated in the presence or absence of EGF (10 ng/ml). *(A, B)* Phase-contrast microscopy images of scratch wounds at baseline and at 24 h. Results are representative of at least two independent experiments. *(C)* The number of migrated keratinocytes 24 h after scraping. Results are expressed as mean ± standard deviation (SD) of three visual fields of wild-type and GnT-V Tg mouse keratinocytes (*$P<0.01$). *(D)* Phase-contrast microscopy images of scratch wounds at 24 h stained by anti-keratin 5 *(green)* and Hoechst 33342 *(blue)*. Bar =50μM *(E)* Phase-contrast microscopy images of scratch wound at 6 h stained by anti-Ki-67 *(red)* and Hoechst 33342 *(blue)*. Bar =50μM *(F)* The ratio of

Ki-67 positive cells to total cells. Results are expressed as mean ± standard deviation (SD) of five visual fields of wild-type and GnT-V Tg mouse keratinocytes (N.S.: not significant).

Fig. 3. EMT-like phenotype was observed in GnT-V Tg mouse keratinocytes. *(A, B, C, D)* Primary cultured keratinocytes derived from wild-type and GnT-V Tg mice were stained with anti-E-cadherin *(A; green)*, anti-N-cadherin *(B; green)* anti-α-SMA *(C, D; green)*, anti-K5 *(D; red)* and Hoechst 33342 *(blue)*. Bar =100μM *(A)*, 50μM *(B, C)*, 25μM *(D)*. *(E)* Expression of E-cadherin in wild-type and GnT-V Tg mouse keratinocytes was assessed by Western blot analysis. Graph show quantification of relative expression of E-cadherin to β-actin. Results are described as mean ± standard deviation (SD) of three independent experiments. (*$P<0.05$) *(F)* Expression of α-SMA and GnT-V in wild-type and GnT-V Tg mouse keratinocytes was assessed by Western blot analysis.

Fig. 4. EMT-like phenotype was observed in the GnT-V Tg mouse keratinocytes. EMT-associated transcriptional factors snail, twist, E-cadherin, and, N-cadherin were evaluated by quantitative RT-PCR, and target gene expression was normalized to GAPDH. Results are expressed as mean ± SD (n=6).

Fig. 5. Increased β1,6 GlcNAc branching on the EGF-R in GnT-V Tg mouse keratinocytes upregulates EGF-R signaling. *(A)* Western blot analysis of EGF-R after L_4-PHA lectin immunoprecipitation of skin specimens from wild-type and GnT-V Tg mice (n=2/each group). Western blot analysis of β-actin (lower panel) showed the same protein concentrations before lectin immunoprecipitation. *(B)* Erk phosphorylation of wild-type and GnT-V Tg mouse keratinocytes was evaluated at the indicated time points (0, 1, 5, 10, 30 min) after stimulation with EGF (10 ng/ml). *(C)* Scrape-wounded, confluent keratinocyte monolayers of wild-type and Tg mice were incubated for 22 h with EGF (10 ng/ml). Bars indicate mean ± standard deviation (SD) of three visual fields of wild-type and GnT-V Tg keratinocytes (*$P<0.01$). *(D)* Scrape-wounded, confluent keratinocyte monolayers of wild-type and GnT-V Tg mice were incubated for 24 h with the EGF-R inhibitor AG1478 (10 ng/ml). Bars indicate mean ± standard deviation (SD) of three visual fields of wild-type and GnT-V Tg keratinocytes (*$P<0.01$). *(E)* Western blot analysis of L_4-PHA and E-cadherin after immunoprecipitation with anti-E-cadherin antibodies from wild-type and GnT-V Tg mouse keratinocytes.

Fig. 6. Enhanced wound healing was observed in GnT-V Tg mice. An 8-mm punch biopsy of skin was obtained from the back of 16-week-old male wild-type and GnT-V Tg mice, and wound closure was monitored (wild-type mice, n=13, Tg mice, n=17) *(A)* Reduction of wound area on days 2, 4, 6, 8, and 10 (*$P<0.05$). *(B)* Macroscopic view of wound healing on day 8 after biopsy. *(C)* Time required for wound closure (days, mean ± SD). *(D)* Expanded photograph of re-epithelialization in wild-type and GnT-V Tg mice on day 6. Dotted lines show the re-epithelialized edge of the epidermis. Bars indicate mean re-epithelialization (distance) on day 6 (*$P<0.05$).

Downloaded from www.jbc.org at OSAKA UNIVERSITY, on July 25, 2011

Figure 1

A

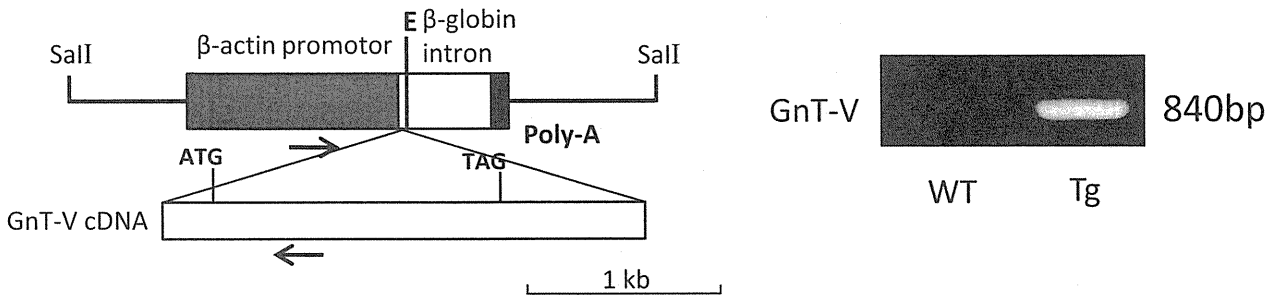

B

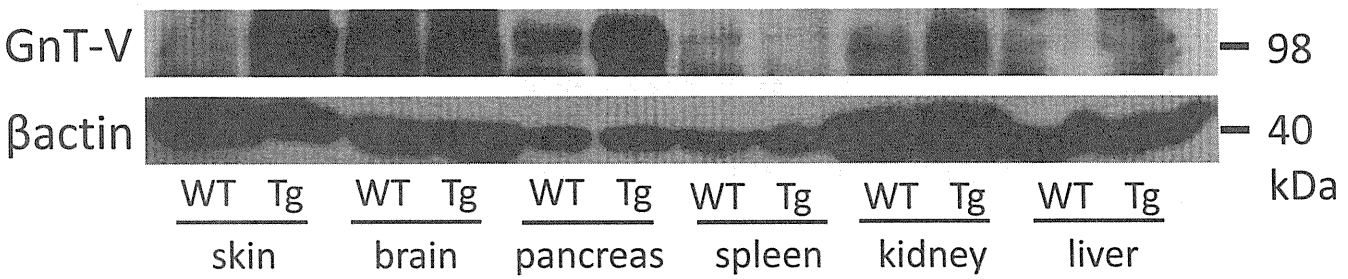

C

GnT-V Activity (pmol / h / mg protein)		
Tissue	WT	Tg
skin	83.3±34.6	492±121
liver	21.3±12.1	46.9±35.8
pancreas	25.4±10.1	1054±127
spleen	77.0±11.2	27.0±6.70
kidney	57.3±10.0	174.1±75.1
brain	71.5±40.6	86.5±12.1

D

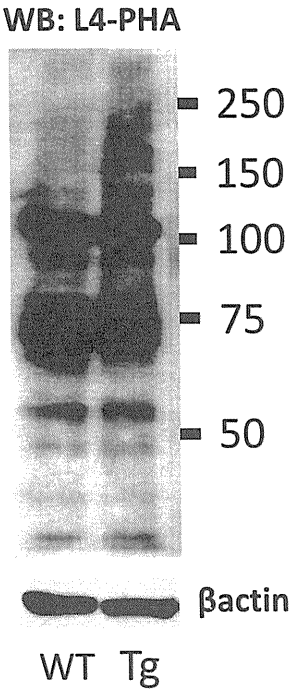

E

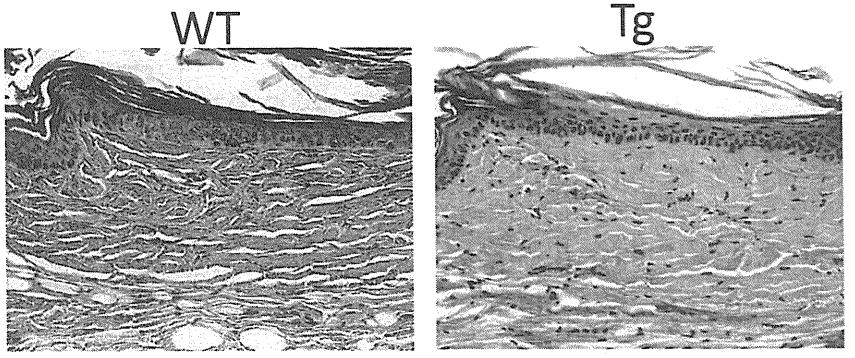

Downloaded from www.jbc.org at OSAKA UNIVERSITY, on July 25, 2011

Figure 2

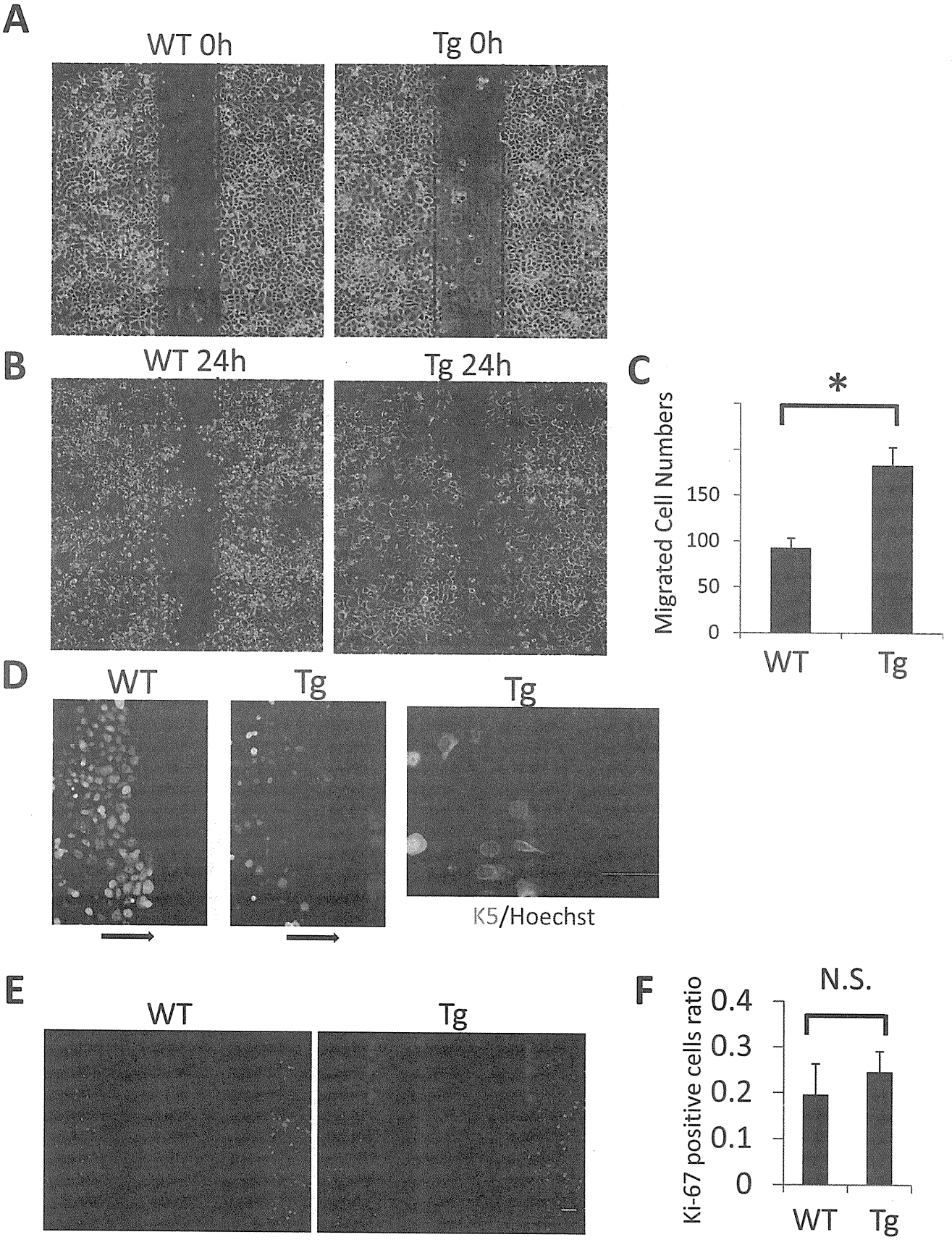

Downloaded from www.jbc.org at OSAKA UNIVERSITY, on July 25, 2011

Figure 3

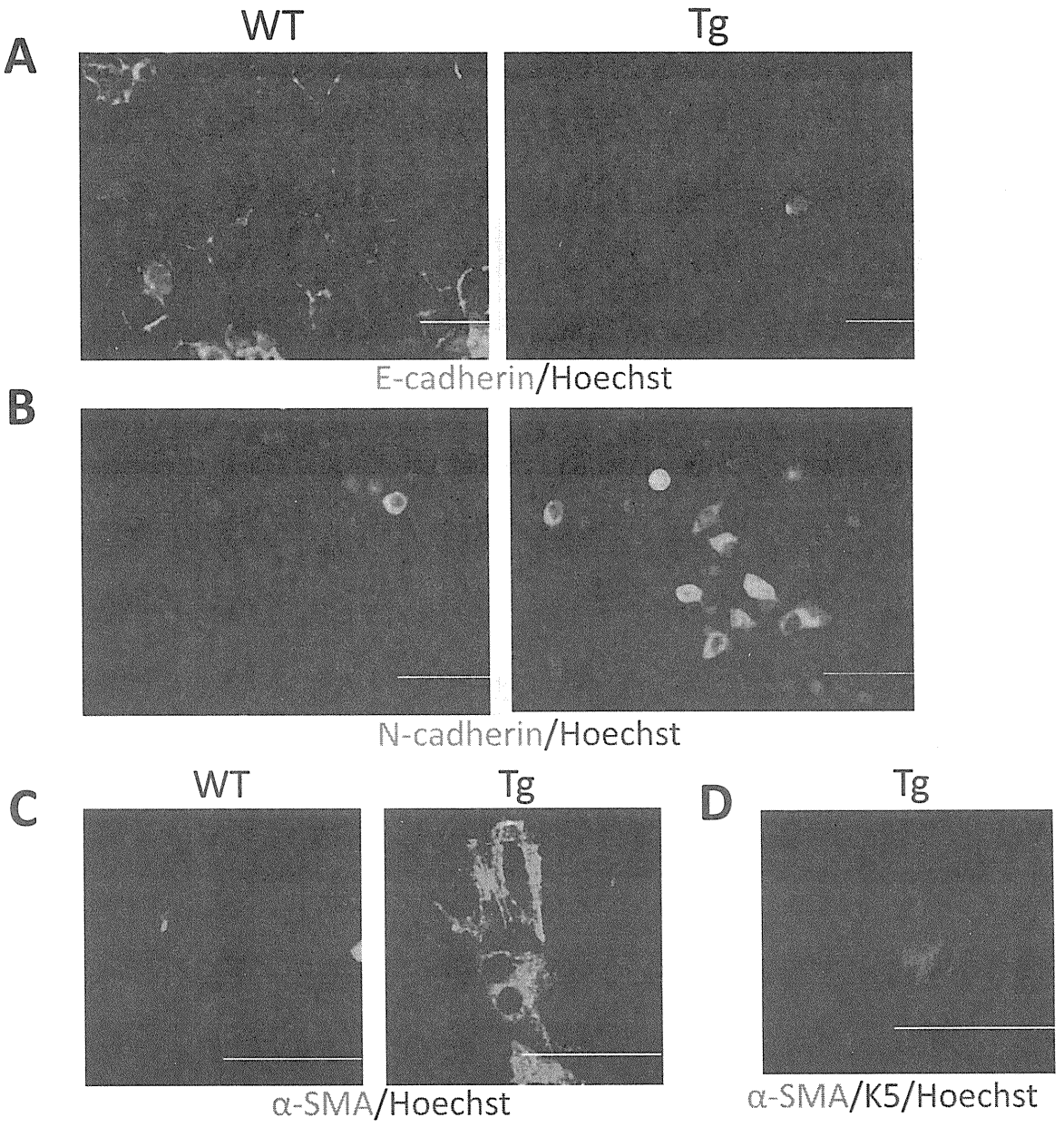

Downloaded from www.jbc.org at OSAKA UNIVERSITY, on July 25, 2011

Figure 4

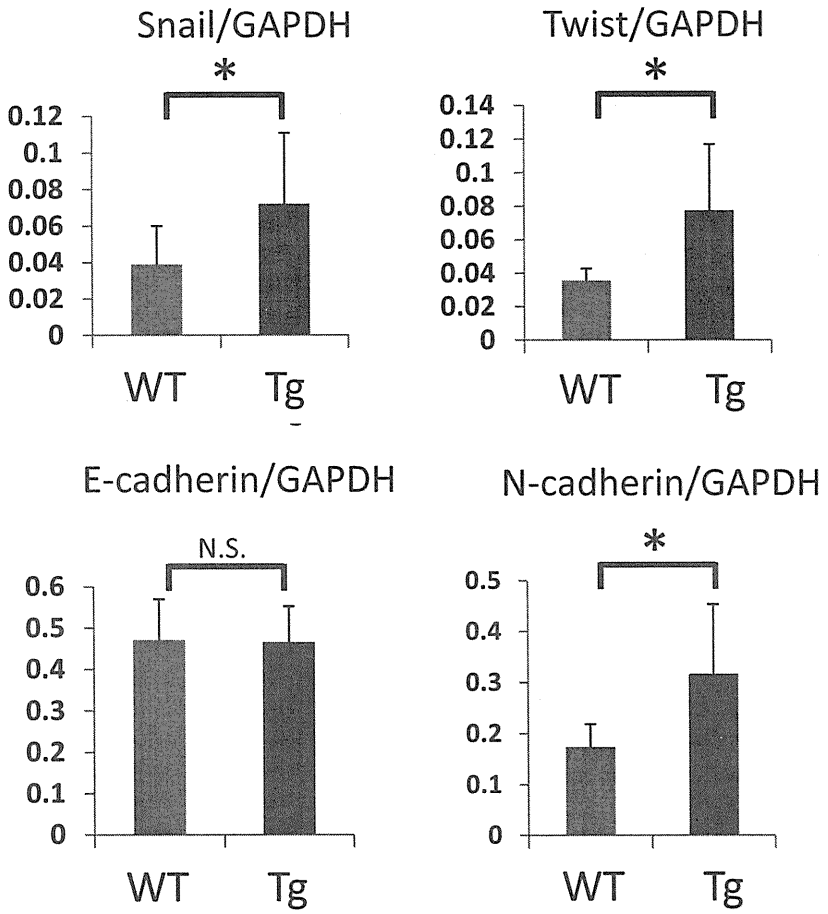

Downloaded from www.jbc.org at OSAKA UNIVERSITY, on July 25, 2011

Figure 5

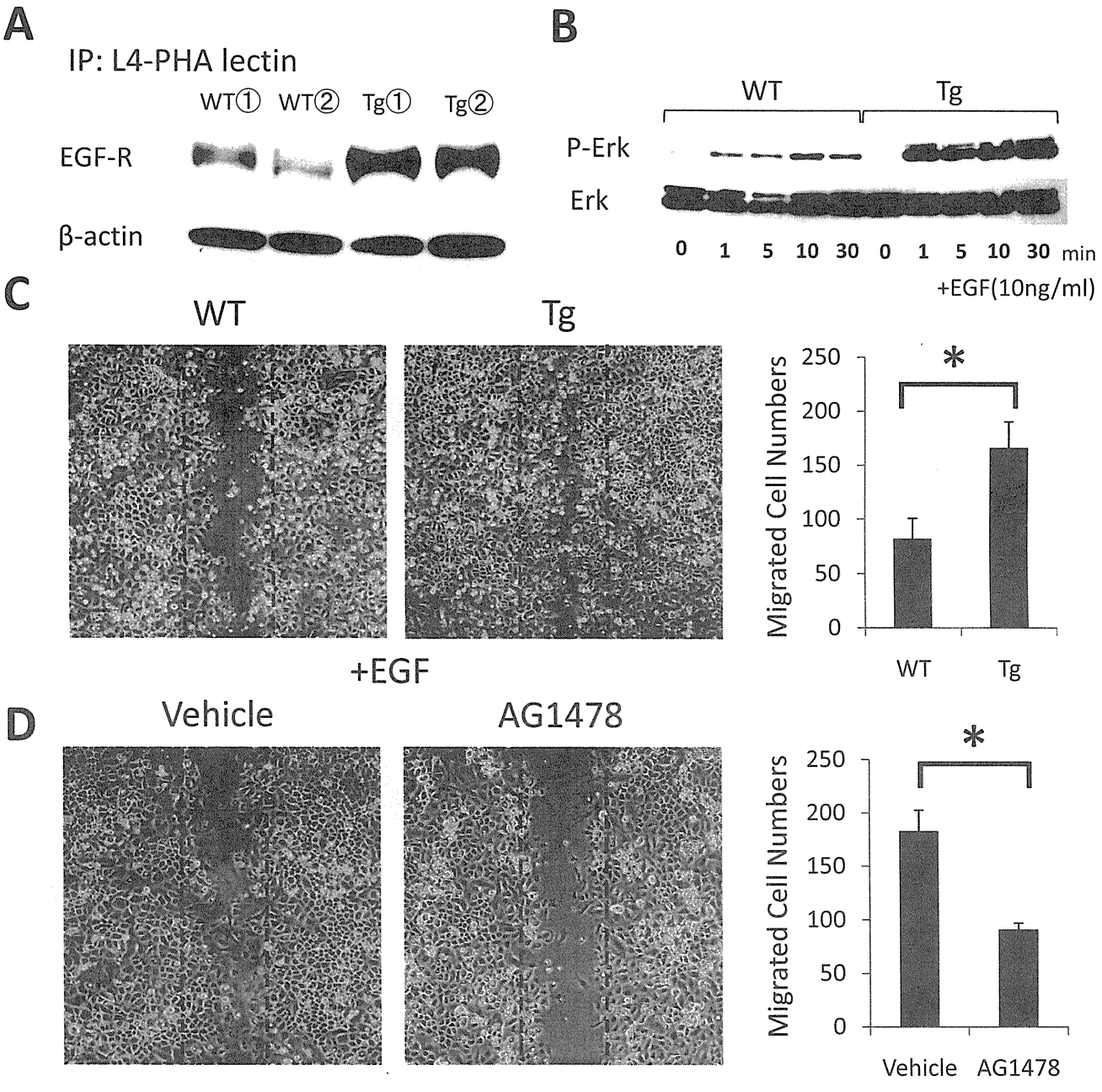

Downloaded from www.jbc.org at OSAKA UNIVERSITY, on July 25, 2011

Figure 6

A

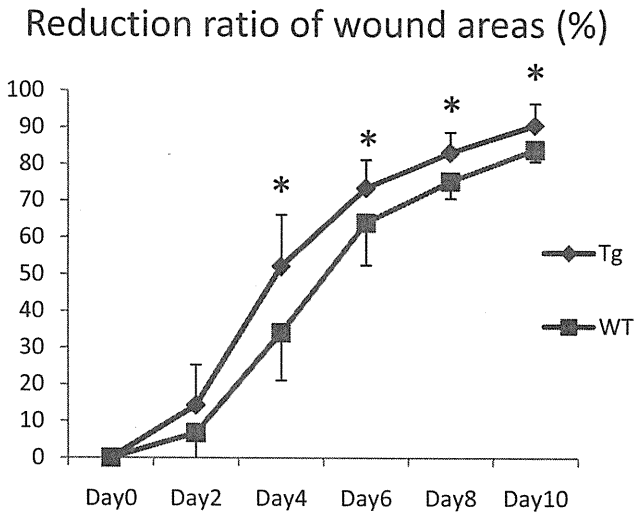

B

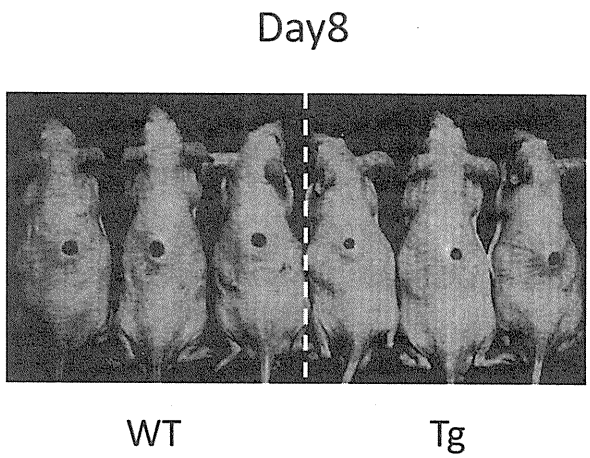

C

average closure date	
WT	16.0±1.81
Tg	14.4±1.91
	P=0.034

D

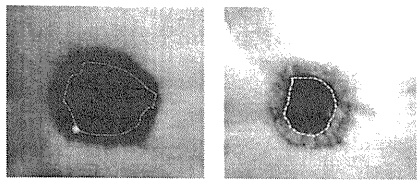

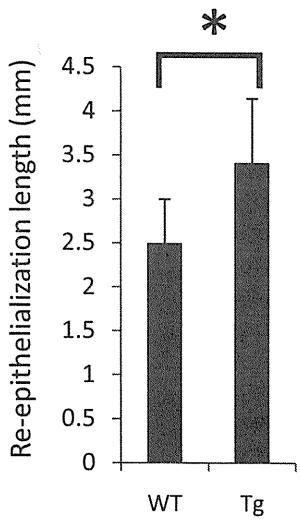

Downloaded from www.jbc.org at OSAKA UNIVERSITY, on July 25, 2011

Case Reports in Dermatology

Case Rep Dermatol 2011;3:107–112
DOI: 10.1159/000328797

Published online: May 17, 2011

© 2011 S. Karger AG, Basel
ISSN 1662–6567
www.karger.com/cde

This is an Open Access article licensed under the terms of the Creative Commons Attribution-NonCommercial-NoDerivs 3.0 License (www.karger.com/OA-license), applicable to the online version of the article only. Distribution for non-commercial purposes only.

Peculiar Distribution of Tumorous Xanthomas in an Adult Case of Erdheim-Chester Disease Complicated by Atopic Dermatitis

Yukako Murakami[a] Mari Wataya-Kaneda[a] Mika Terao[a]
Hiroaki Azukizawa[a] Hiroyuki Murota[a] Yukiko Nakata[b]
Ichiro Katayama[a]

Departments of [a]Dermatology and [b]Clinical Laboratory Diagnostics, Osaka University Graduate School of Medicine, Osaka, Japan

Key Words
Erdheim-Chester disease · Hand-Schüller-Christian disease · Xanthoma · Atopic dermatitis · Macrophage · CD68 · CD163 · Thymus- and activation-regulated chemokine

Abstract
Erdheim-Chester disease is a rare non-Langerhans form of histiocytosis with multiple organ involvement. Approximately 20% of patients have xanthoma-like lesions, usually on the eyelids. We report a case of Erdheim-Chester disease in a 32-year-old male who showed peculiar xanthomatous skin lesions and also had atopic dermatitis. His skin manifestations included ring-like yellowish tumors on his periorbital regions, rope necklace-like tumors on his neck, and spindle-shaped tumors on his right preauricular region and cubital fossas. He also had exophthalmos and diabetes insipidus. Chronic eczematous lesions were present on the flexor aspect of his extremities, and his serum eosinophil numbers and immunoglobulin E levels were elevated. A histological examination of his right neck tumor showed foamy macrophages and touton-type giant cells, which were positive for CD68 and CD163 and negative for S-100 and CD1a. We suggest that the complication of atopic dermatitis may have contributed to the uncommon clinical features in this case.

Case Report

A 32-year-old male presented with xanthomatous skin lesions, exophthalmos, and diabetes insipidus. His left retro-orbital mass was partially removed in childhood at another hospital, and he had been diagnosed with Hand-Schüller-Christian disease (HSCD). His past medical history included hyperlipidemia, type 2 diabetes mellitus, hypertension, and hyperuricemia, which were managed with

Yukako Murakami, MD
Department of Dermatology
Osaka University Graduate School of Medicine
2-15 Yamadaoka, Suita-City, Osaka 565-0871 (Japan)
Tel. +81 6 6879 3031, E-Mail murakami@derma.med.osaka-u.ac.jp

KARGER